Order reduction for a signaling pathway model of neuronal synaptic plasticity

Mikko Lehtimäki [*,***] **Lassi Paunonen** [**] **Seppo Pohjolainen** [**] **Marja-Leena Linne** [*,***]

[*] *Computational Neuroscience Group, BioMediTech Institute and Faculty of Biomedical Sciences and Engineering, Tampere University of Technology, FI-33720 Tampere, Finland (email: lehtimaki.mikko@gmail.com, marja-leena.linne@tut.fi)*
[**] *Mathematics, Faculty of Natural Sciences, Tampere University of Technology, Tampere, Finland, FI-33720 Tampere, Finland (email: lassi.paunonen@tut.fi, seppo.pohjolainen@tut.fi)*
[***] *Department of Signal Processing, Tampere University of Technology, FI-33720 Tampere, Finland*

Abstract: In this study a nonlinear mathematical model of plasticity in the brain is reduced using the Proper Orthogonal Decomposition and Discrete Empirical Interpolation Method. Such methods are remarkably useful for connecting reduced small scale models via the inputs and outputs to form optimally performing large scale models. Novel results were obtained as mathematical model order reduction has not been applied in neuroscience without linearization of the mathematical model and never to the model presented here. The reduced order model consumes considerably less computational resources than the original while maintaining a low root mean square error between the original and reduced model.

Keywords: model reduction, nonlinear models, Proper Orthogonal Decomposition, Discrete Empirical Interpolation Method, cell signaling, synaptic plasticity

1. INTRODUCTION

Dimensionality reduction is a commonly used method in engineering sciences, such as control theory, in improving computational efficiency of simulations of complex nonlinear mathematical models. In the field of neuroscience, there is a great demand to incorporate molecular and cellular level detail in large-scale models of the brain in order to reproduce phenomena such as learning and behavior. This cannot be achieved with the computing power available today, since the detailed models are complex and often computationally too demanding for large-scale network or system level simulations.

In the field of systems biology, models are typically simplified by completely eliminating variables, such as molecular entities, from the system, and making assumptions of the system behavior, for example regarding the steady state of the chemical reactions. However, this approach is not suitable for the current trend in neuroscience, in which multiple physical scales of the brain are incorporated in simulations and the consequent analysis of neural phenomena. Instead comprehensive models with full system dynamics are needed in order to increase understanding of different actors in one brain area.

The information loss typically induced by eliminating variables of the system can be avoided by mathematical reduction methods that strive to approximate the entire system with a smaller number of dimensions compared to the original system. Here we demonstrate the effectiveness of mathematical model order reduction methods in approximating the behavior of all the variables in the original system by simulating a model with a radically reduced dimension.

In this study, mathematical model reduction is applied in the context of an experimentally verified signaling pathway model of plasticity. This nonlinear chemical equation based data-driven model was published in Kim et al. (2013), and it describes the biochemical calcium signaling steps required for plasticity, and hence for learning, in the subcortical area of the brain. In addition to nonlinear characteristics, the model includes time-dependent terms, which pose an additional challenge both computational efficiency and reduction wise. The chosen biophysical model is one of the most comprehensive models out of those that are currently able to explain aspects of plasticity on the molecular level with chemical interactions and the law of mass action. The original model is too detailed for utilization in large-scale network simulations, which serves as motivation for the present study. Moreover, with this case study the aim is to demonstrate that the behavior of the model can be analysed faster yet with satisfactory accuracy by using a reduced order model.

The model order reduction method employed in this study is Proper Orthogonal Decomposition with Discrete Empirical Interpolation Method (POD+DEIM), a subspace projection method for reducing the dimensionality of nonlinear systems. By applying these methods, the simulation time of the plasticity model is radically compressed al-

though approximation errors are present if the model is reviewed on large time scales. The tolerated amount of approximation error depends on the final application of the model. Based on these promising results, POD+DEIM are recommended for dimensionality reduction in computational neuroscience.

Algorithms to achieve the elimination-type reduction for nonlinear neuronal models have been proposed for instance in Woo et al. (2005), Sorensen and DeWeerth (2006) and later in Shin et al. (2009). However the studies rely on several assumptions of the model structure and are only suitable in very specific scenarios. Recently, a variable elimination strategy was used to reduce a model of astrocyte metabolism in Diekman et al. (2013). Additionally, mathematical reduction of neuronal dendrite using a linearization approach has been performed in Kellems et al. (2009) and a nonlinear model discretized from partial differential equations has been reduced in Du et al. (2014).

An empirical interpolation method for reducing the complexity of nonlinear functions was first proposed by Barrault et al. (2004). The discrete version Discrete Empirical Interpolation Method (DEIM) was then introduced in Chaturantabut and Sorensen (2010). The previous five years have seen DEIM developed further with localized, adaptive and stability conserving variants in Peherstorfer et al. (2014); Peherstorfer and Willcox (2015); Amsallem and Nordström (2016) as well as a monotonicity preserving variation for reaction diffusion systems in Chaturantabut (2016). DEIM is a method that complements POD by reducing the nonlinear term so that together the two arrive at a reduced model which no longer depends on the original dimension of the system. Alternatively, DEIM can be used for standalone reduction of nonlinear functions.

2. PLASTICITY MODEL

We study a mathematical model of signaling pathways in striatal synaptic plasticity by Kim et al. (2013). The model is specific for the basal ganglia area of the brain and it describes how certain molecules in intercellular information transfer points of neurons, synapses, are responsible for plasticity, which is presumably a prerequisite for learning in the brain. It is a biophysicochemical model that is based on experimental data. Originally the model was employed in studying the effects of different stimuli to the synapse and how they could direct plasticity. Additionally, the predictions from the model have been verified experimentally and the model itself is based on validated experimental data.

The model is based on chemical reactions of the molecules in the synapse. The stoichiometric equations obey the law of mass action, which leads to a deterministic system of ordinary differential equations. Our implementation of the model contains $n = 44$ ordinary differential equations.

The model has two external stimulus variables, calcium ion (Ca) and neurotransmitter glutamate (Glu). The state-space model is of the form

$$\begin{aligned}\dot{x}(t) =& A(t)x(t) + F(x(t)) + B \cdot Glu(t)\\ =& (A_0 + A_1 Ca(t) + A_2 Ca(t)^2 + A_3 Glu(t))x(t) + \\ & F(x(t)) + B \cdot Glu(t)\end{aligned} \quad (1)$$

and the system is nonautonomous due to a Ca stimulus being part of $A(t)$. In our simulations, both Ca and Glu stimuli are fixed functions in the model reduction and testing phases. If Glu and Ca are considered inputs to the system, the result is a nonlinear control system, which additionally has bilinear characteristics. The five first equations of the model are

$$\begin{aligned}\dot{x}_1 =& k_{prodAG_c} \cdot x_4 - k_{degAG_f} \cdot x_1\\ \dot{x}_2 =& k_{PMCA_c} \cdot x_{15} + k_{NCX_c} \cdot x_{11} - k_{Leak_f} \cdot x_2 \cdot x_{36} + \\ & k_{Leak_b} \cdot x_{10}\\ \dot{x}_3 =& k_{buffer_f} \cdot Ca(t) \cdot x_{19} - k_{buffer_b} \cdot x_3\\ \dot{x}_4 =& k_{prodAG_f} \cdot x_{21} \cdot x_7 - k_{prodAG_b} \cdot x_4 - k_{prodAG_c} \cdot x_4\\ \dot{x}_5 =& k_{DAG_3c} \cdot x_8 - k_{DAG_4f} \cdot x_5,\end{aligned} \quad (2)$$

and they illustrate the nonlinearity of the system in equation of $\dot{x}_2$, and the time-dependence of the system in the equation of $\dot{x}_3$. In Equation (2), terms k_n represent constants and x_n chemical species. This nonlinear system has a sparse linear part and includes a time dependent stimulus. In the numerical implementation of the model, the linear coefficients, nonlinear function and external inputs of the system are separated.

For the following analysis five biologially interesting species included in the model were chosen as outputs of the system to be studied in more detail. These were 2-arachidonoylglycerol ($\mathrm{Ag_{post}}$), external calcium ($\mathrm{Ca_{ext}}$), diacylglycerol ($\mathrm{DAG_{post}}$), G protein with α, β and γ subunits ($\mathrm{Gabg_{post}}$) and phospholipase C ($\mathrm{PLC_{post}}$). In the present model these species are also included as state variables. Their behavior is significant as these substances can connect the current model to a larger, even more detailed model and they are known to be active influencers in the two forms of plasticity, LTP (long term potentiation) and LTD (long term depression) (see Manninen et al. (2010); Hellgren-Kotaleski and Blackwell (2010)).

3. MODEL REDUCTION USING POD AND DEIM

In this section we outline the Proper Orthogonal Decomposition (POD) (see Lumley et al. (1993); Sirovich (1987); Kellems et al. (2009, 2010); Benner et al. (2015)) and Discrete Empirical Interpolation Method (DEIM) (see Chaturantabut and Sorensen (2010)) that are used to reduce the order of the quadratic and nonautonomous model discussed in Section 2. POD is a well-known method that is used in model reduction of various types of differential equations, partial differential equations and dynamical systems.

The underlying idea of the POD method is to project the system (1) onto a subspace so that the reduced system approximates the dynamical behaviour of (1) in the best possible way in the sense of least squares. The POD reduction procedure is begun by simulating the full system (1) and choosing "snapshots" $x(t_j)$ of the state of the system at equally spaced time instances $(t_j)_{j=1}^{N_s} \subset [0, T]$ where $T > 0$ is the length of the time interval (see Sirovich (1987)). The POD reduction replaces the system (1) with an approximate system on the space spanned by the first $1 \leq k \leq n$ singular vectors of the matrix $S = [x(t_1), \ldots, x(t_{N_s})] \in \mathbb{R}^{n \times N_s}$. In particular, if

$S = V\Sigma W^*$ is the singular value decomposition of S and V_k consists of the first k columns of V, then the POD reduced order model of (1) has state $x_k(t) = V_k^* x(t)$, and its dynamics are determined by the Galerkin projection

$$\dot{x}_k(t) = V_k^* A(t) V_k x_k(t) + V_k^* F(V_k x_k(t)) + V_k^* B u(t), \quad (3)$$

where $u(t)$ is the input vector.

The main drawback of the reduced model (3) in terms of computational efficiency is that the function $F(V_k x_k(t))$ appearing in the nonlinear term needs to be evaluated for a full-sized vector $V_k x_k(t) \in \mathbb{R}^{n\times n}$ with $n = 44$. The computational cost of evaluating the nonlinear term can be reduced by approximating the function F using the DEIM procedure.

DEIM extends POD with an interpolation step for nonlinear terms of the model, while also maintaining a subspace projection approach. The construction of the DEIM approximation begins with the construction of the so-called *DEIM modes*, vectors $U_m = [u_1, ..., u_m] \in \mathbb{R}^{n\times m}$. The matrix U_m consists of the first $m \leq n$ left-singular vectors of the matrix $[F(x(t_0)), \ldots, F(x(t_{N_s}))]$ (these columns of the DEIM projection matrix can be collected during the generation of the snapshots in the POD reduction process to minimize offline computational burden of DEIM).

In the second step of the DEIM procedure we define

$$P = [e_{\wp_1}, ..., e_{\wp_m}] \in \mathbb{R}^{n\times m}, \quad (4)$$

where $e_{\wp_j} \in \mathbb{R}^n$ are the columns of the identity matrix $I \in \mathbb{R}^{n\times n}$ and where $\{\wp_1, ..., \wp_m\}$ is a set of *interpolation indices*. The indices $\{\wp_1, ..., \wp_m\}$ are chosen based on the columns of U_m using the algorithm presented in (Chaturantabut and Sorensen, 2010, Algorithm 1). By construction the matrix $P^T U_m \in \mathbb{R}^{m\times m}$ is nonsingular.

The function $F : \mathbb{R}^n \to \mathbb{R}^n$ is of the form $F(x) = [f_1(x), \ldots, f_n(x)]^T$, where $f_j : \mathbb{R}^n \to \mathbb{R}$ for $j \in \{1, \ldots, n\}$. We define $F_m : \mathbb{R}^n \to \mathbb{R}^m$ such that $F_m(x) = [f_{\wp_1}(x), \ldots, f_{\wp_m}(x)]^T$. Finally, the DEIM approximation of the nonlinear term $F(V_k x_k(t))$ in the POD approximation is given by

$$F_{(k,m)}(V_k x_k(t)) = V_k^T U_m (P^T U_m)^{-1} F_m(V_k x_k(t)), \quad (5)$$

where the matrix $V_k^T U_m (P^T U_m)^{-1} \in \mathbb{R}^{k\times m}$ can be computed in the offline stage. The computational savings of the DEIM approximation result from the fact that in the function $F_{(k,m)}(\cdot)$ we only need to evaluate m component functions of the original nonlinear function $F(\cdot)$.

The final reduced order form of the system (1) becomes

$$\dot{x}_k(t) = A_k(t) x_k(t) + F_{(k,m)}(V_k x(t)) + B_k u(t),$$

where $x_k(t) = V_k^* x(t)$, $A_k(t) = V_k^* A(t) V_k$, $B_k = V_k^* B$, and $F_{(k,m)}$ is defined in (5).

The orders k and m of the POD and DEIM model reductions can be chosen independently of each other.

4. SIMULATION RESULTS

In order to compare the original model versus POD+DEIM reduced models the simulation speed and error of several subspace dimensions were measured. The original and reduced ordinary differential equation systems were simulated in Matlab for time span $t = [0, 10000]$ using the variable time step ODE15S solver for stiff differential equations. For each POD dimension $k = 2 : 2 : 40$ (Matlab notation), DEIM dimension $m = 5 : 5 : 30$ reduced models were calculated. For each combination, 20 simulations were performed and their average computation times and system solutions at each time step were stored.

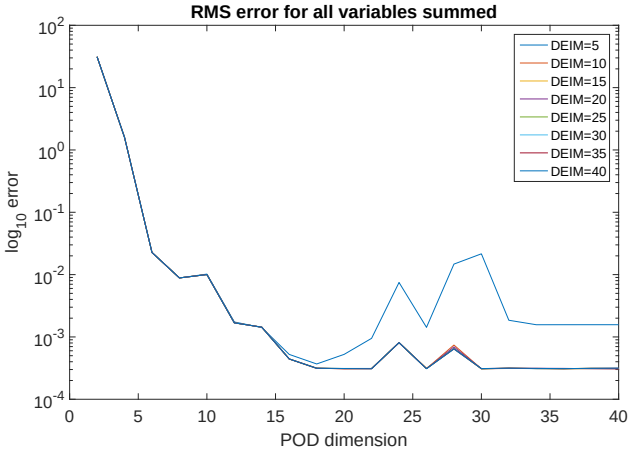

Fig. 1. Root mean square error between the original model and reduced order solutions. X-axis shows POD dimension and y-axis the error on logarithmic scale. Each distinctly colored plot corresponds to different dimensions used in DEIM.

Figure 1 shows the root mean square (RMS) error between the full dimension model and different reduced models of each POD+DEIM combination. The y-axis contains the error values on a logarithmic scale, while x-axis indicates the number of POD dimensions. Each line in the plot corresponds to a DEIM dimension. RMS error was calculated by

$$e_{RMS} = \sqrt{\frac{1}{k}\sum_{n=1}^{k}(Y - \tilde{Y})^2} \quad (6)$$

where Y is the matrix of solutions of the original system, $\tilde{Y} = V_k Y_{reduced}$ is the matrix of reduced order simulation results transformed back into the original space and k is the number of elements in the matrices.

From Figure 1 it is seen that regardless of the DEIM mode, or the nonlinear dimensionality, the error decays exponentially until POD dimension 15 is reached. This suggests that more than 15 POD dimensions is not necessary beneficial for a reduced order model, since the accuracy will not improve with additional dimensions. Depending on the application, as little as five to ten dimensions could be sufficient for simulating this model while keeping the error tolerable. Moreover the RMS error is seen to not depend radically on the DEIM dimension. Increasing the DEIM modes from 5 to 10 reduces the error if the POD mode is already over 15. This suggests that the linear part of the model that is reduced with POD is dominant in terms of approximation error and that the interpolation approach to reducing the nonlinear complexity is effective.

Figure 2 displays the relative computational advantage gained from the reduced model in terms of simulation speed. In the figure, the simulation time of the original full dimension model is plotted as a straight red line. From Figure 2 it is seen that the simulation time is

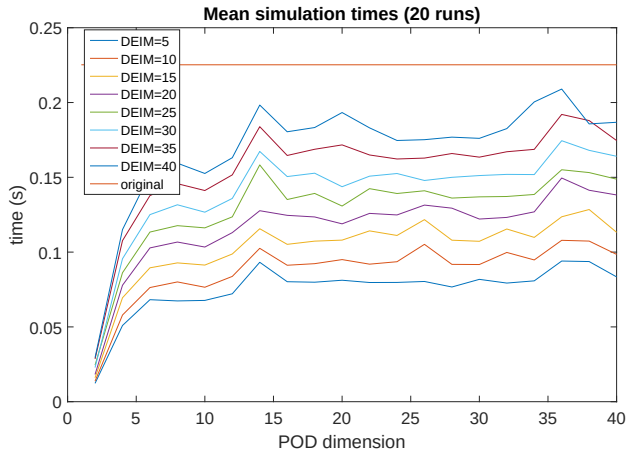

Fig. 2. Mean simulation times of 20 executions of each POD+DEIM reduced model compared to the original model, plotted as a straight red line. The y-axis shows the simulation time in seconds, and x-axis shows the POD dimension. Each colored plot corresponds to a DEIM dimension. Simulation time interval was $t = [0, 10000]$.

approximately halved by using 20 DEIM modes, which corresponds to halving the original dimension (44) of the nonlinear term. The simulation times depend on POD reduction only when less than 15 modes are chosen. In summary, for this model, the nonlinear term is the largest computational burden, since reducing it has the largest effect on simulation times.

Figure 3 displays how the dynamics of selected output species given by the reduced order model (red line) compared to the original model (blue line) in the first 5000 seconds. Here y-axis shows the concentration of each substance and x-axis the time. Analyzing the solutions in this format is important, for the absolute error measured earlier does not take into account how the error as a function of time is affected by dimension reduction. In the context of neural models, it is important that the dynamics are preserved. For example, information transmission via calcium signaling between astrocytes and neurons has been demonstrated to be amplitude and frequency modulated in Wade et al. (2011), so even a slight defect might cause the higher level behavior of the model to change.

The concentrations of molecular species participating in specific signaling pathways are difficult, or sometimes impossible to measure, which emphasizes the importance of modeling the dynamics of signaling pathways. The experimental challenge is related to measurement techniques: to this day there is no direct way to estimate the exact concentrations of molecular entities in as a function of time nor the possible variability of molecular entities. The changes in concentrations are measured, as an example, using fluorescent Ca^{2+} indicators which do not directly give absolute concentrations. For some of the variables described in this study, such as the calcium, some estimates of measures can however be obtained from theoretical studies. The average volume of a spine is 1 fl and resting level concentration of Ca^{2+} is 0.1 μM, which means that there are about 60 calcium ions in one spine. Moreover, it has been estimated that when 100 calcium ions enter into the spine head, it increases the calcium concentration in the spine from 100 to 300 nM (depending on the volume of the spine), which corresponds to the physiological range of increases (see Majewska et al. (2000); Holcman et al. (2004)).

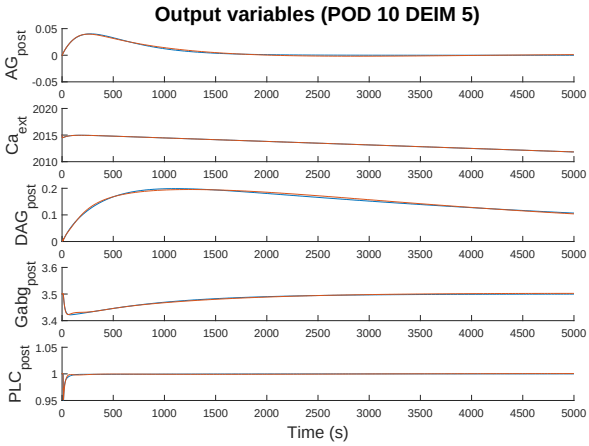

Fig. 3. Solutions of the dynamics of the selected biologically interesting output variables. Five species were tracked and their behavior plotted as a function of time. The y-axis displays the concentration of each ion/molecule. Blue line is the original model, and red is the approximation from the reduced order model with 10 POD and 5 DEIM modes.

However, the reduced order is not able to predict the behavior of the system when a simulation time longer than the training time is used. In order to test whether a low number of POD modes would be able to perform a near-correct approximation for a very long time span if the snapshots were also taken from a prolonged simulation, new reduced models were generated. The employed simulation time was $5 * 10^9$ seconds. Figure 4 shows the approximation with 10 POD and 5 DEIM modes and it is seen that $Gabg_{post}$ and PLC_{post} significantly different from the correct solution. However, a very good approximation was obtained with 30 POD and 10 DEIM modes, which is seen in Figure 5, while almost maintaining a simulation time of one third of the original model. The reduced model has gained more pronounced oscillations, although their amplitude is extremely low. Moreover, the steady state concentrations are physiologically very close to the original and in an acceptable range considering the inherent errors a deterministic model such as the one studied here always has. Whether the errors seen here would affect the behavior of a multi-scale model remains a question for another study.

The magnitude of the errors with a long simulation time was further studied using the absolute and relative errors between the original model and the 30 POD 10 DEIM reduced model. The errors are visualized in Figure 6 and Figure 7. The absolute errors are small, with the size being less than 10^{-6} for all species except calcium, where the range is approximately 10^{-2}. The relative errors for PLC and $Gabg$ confirm that the observed variation is extremely small. The relative errors for AG, Ca_{ext} and DAG on the other hand display oscillations in the reduced order model and additionally, are in a different magnitude than

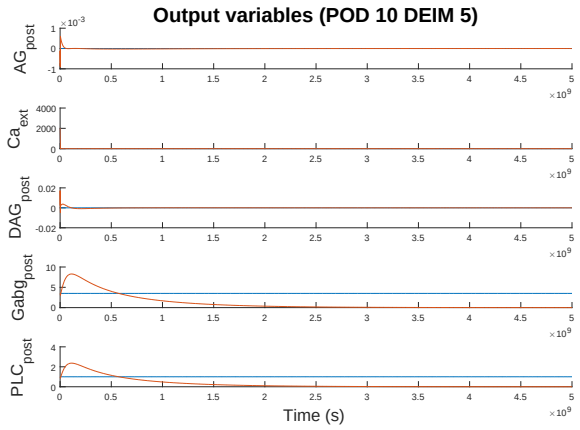

Fig. 4. Behavior the reduced order model in a long duration simulation using ten POD and five DEIM modes. Blue line is the original model and red is the reduced model for each output variable. The simulation time was $5 * 10^9$ seconds.

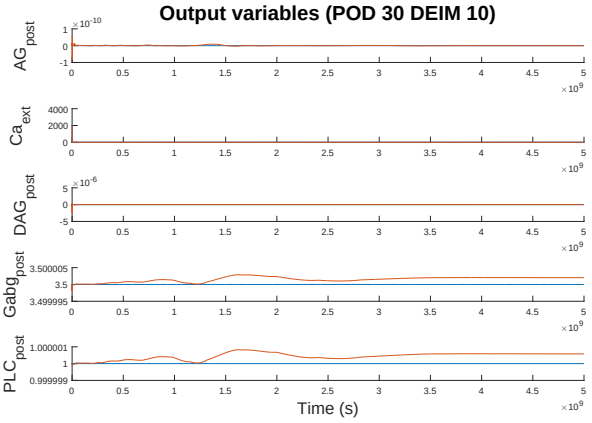

Fig. 5. Behavior the reduced order model in a long duration simulation using 30 POD and 10 DEIM modes. Blue line is the original model and red is the reduced model for each output variable. The simulation time was $5 * 10^9$ seconds.

the two other output species, achieving 10^8. However, the magnitude can be explained by numerical inaccuracy of the denominator, since the true concentration reaches zero at all points where a high error is seen, except at the very beginning of the simulation where stimulus is applied. Moreover, the relative error indicates that these three species correctly predict the steady state concentration, eventually, seen as the error degrading to zero.

To conclude, good results are achieved when the reduced order model is trained in a matching time interval to the final use case. The greatest challenge for the present method is generalizing the reduced model to longer time intervals. This issue is possibly solved by more recent improvements of the DEIM algorithm introduced in Peherstorfer et al. (2014) and Peherstorfer and Willcox (2015).

5. CONCLUSIONS

In this study Proper Orthogonal Decomposition and Discrete Empirical Interpolation Method (POD+DEIM) was

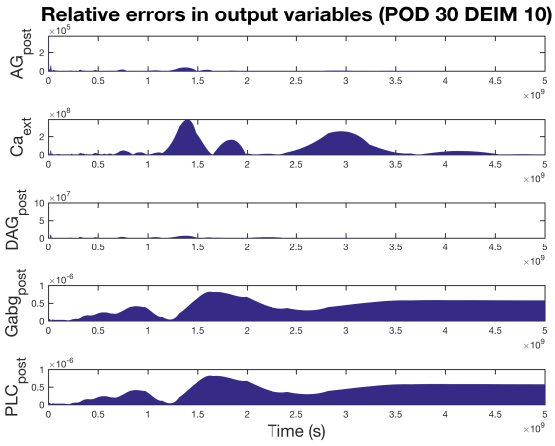

Fig. 6. Relative error between the 30 POD and 10 DEIM modes reduced model and the original model at every 10^6 seconds when simulated for $5 * 10^9$ seconds.

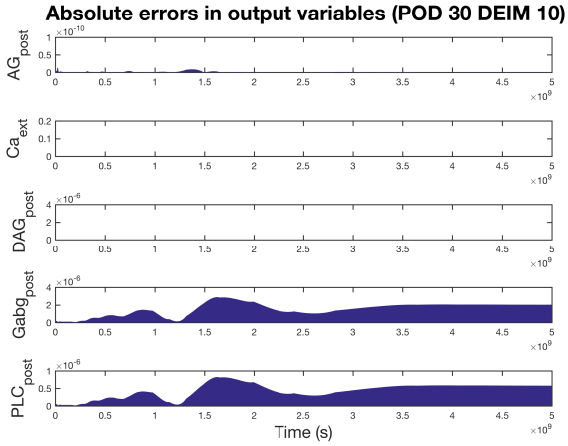

Fig. 7. Absolute error between the 30 POD and 10 DEIM modes reduced model and the original model at every 10^6 seconds when simulated for $5 * 10^9$ seconds.

applied to a data-driven biological model of plasticity in the brain. Five important molecules and ions were chosen for analysis, since these species have the greatest potential to link the model to a larger system comprising more brain areas and features of the multi-scale neural system.

Model order reduction is an essential process for improving the scale and quality of future computational models of the brain. Moreover, reduction methods will become increasingly important when models representing other mammalian species, such as rat and mouse, will be extended into human models. Although many methods of model reduction exist, subspace projection methods show most promise for they can be automatically applied, have adjustable error bounds and scale to virtually any size of system without compromising variables in the model. Additionally, they are applicable to nonlinear systems, either directly or via linearization, which greatly increases their applicability to complex models in neuroscience.

Model reduction with POD+DEIM was found to significantly reduce the simulation time. An additional benefit is that the approximation can be tuned by adjusting the POD and DEIM dimensionality independently. However,

the reduced order model did not achieve a perfect reproduction of the solutions of the original model in long time intervals and the steady states also had slight deviations from the original model. Whether the observed error is tolerable depends on the final purpose of the model.

DEIM has already been developed further and future studies are needed to test the effectiveness of these new variations of the algorithm. The recently published Localized DEIM looks extremely promising for maintaining a low number of approximation modes for widely varying model parameters, given that the conditions were present in the offline training phase of POD+DEIM (Peherstorfer et al. (2014)). Moreover, the adaptive version ADEIM is able to react to unanticipated behavior on the online stage of a simulation by efficiently querying the original system (Peherstorfer and Willcox (2015)). All in all, subspace projection methods seem suitable for reducing the dimensionality of signaling pathway models in neuroscience.

ACKNOWLEDGEMENTS

This project has received funding awarded to M.-L.L from the European Union Seventh Framework Programme (FP7) under grant agreement no 604102 (HBP RUP) and the European Union's Horizon 2020 Research and Innovation Programme under Grant Agreement No. 720270 (HBP SGA1).

L.P. is funded by the Academy of Finland, Grant No. 298182.

REFERENCES

Amsallem, D. and Nordström, J. (2016). Energy stable model reduction of neurons by nonnegative discrete empirical interpolation. *SIAM Journal on Scientific Computing*, 38(2), B297–B326. doi:10.1137/15M1013870.

Barrault, M., Maday, Y., Nguyen, N., and Patera, A. (2004). An empirical interpolation method: application to efficient reduced-basis discretization of partial differential equations. *Comptes Rendus Mathematicue*, 339(9), 667–672. doi:10.1016/j.crma.2004.08.006.

Benner, P., Gugercin, S., and Willcox, K. (2015). A survey of projection-based model reduction methods for parametric dynamical systems. *Society for Industrial and Applied Mathematics Review*, 57(4), 483–531. doi:10.1137/130932715.

Chaturantabut, S. (2016). Nonlinear reduced-order modeling with monotonicity property. In *American Institute of Physics Conference Proceedings*, 2849–2856. AIP Publishing. doi:10.1063/1.4965383.

Chaturantabut, S. and Sorensen, D. (2010). Nonlinear model reduction via discrete empirical interpolation. *SIAM Journal of Scientific Computing*, 32(5), 2737–2764. doi:10.1137/090766498.

Diekman, C., Fall, C., Lechleiter, J., and Terman, D. (2013). Modeling the neuroprotective role of enhanced astrocyte mitochondrial metabolism during stroke. *Biophysical Journal*, 104(8), 1635–1838.

Du, B., Sorensen, D., and Cox, S. (2014). Model reduction of strong-weak neurons. *Frontiers in Computational Neuroscience*, 8(164).

Hellgren-Kotaleski, J. and Blackwell, K. (2010). Modelling the molecular mechanisms of synaptic plasticity using systems biology approaches. *Nature Reviews Neuroscience*, 11, 239–251. doi:10.1038/nrn2807.

Holcman, D., Schuss, Z., and Korkotian, E. (2004). Calcium dynamics in dendritic spines and spine motility. *Biophysical Journal*, 87(1), 81–91. doi:10.1529/biophysj.103.035972.

Kellems, A., Chaturantabut, S., Sorensen, D., and Cox, S. (2010). Morphologically accurate reduced order modeling of spiking neurons. *Journal of Computational Neuroscience*, 28(3). doi:10.1007/s10827-010-0229-4.

Kellems, A., Roos, D., Xioa, N., and Cox, S. (2009). Low-dimensional, morphologically accurate models of subthreshold membrane potential. *Journal of Computational Neuroscience*, 27(2), 161–176.

Kim, B., Hawes, S., Gillani, F., Wallace, L., and Blackwell, K. (2013). Signaling pathways involved in striatal synaptic plasticity are sensitive to temporal pattern and exhibit spatial specificity. *PLoS Computational Biology*, 9(3). doi:10.1371/journal.pcbi.1002953.

Lumley, J., Berkooz, G., and Holmes, P. (1993). The Proper Orthogonal Decomposition in the analysis of turbulent flows. *Annual Review of Fluid Mechanics*, 25, 539–575. doi:10.1146/annurev.fl.25.010193.002543.

Majewska, A., Brown, E., Ross, J., and Yuste, R. (2000). Mechanisms of calcium decay kinetics in hippocampal spines: role of spine calcium pumps and calcium diffusion through the spine neck in biochemical compartmentalization. *Journal of Neuroscience*, 20(5), 1722–1734.

Manninen, T., Hituri, K., Hellgren-Kotaleski, J., Blackwell, K., and Linne, M. (2010). Postsynaptic signal transduction models for long-term potentiation and depression. *Frontiers in Computational Neuroscience*, 4(152), 1–29. doi:10.3389/fncom.2010.00152.

Peherstorfer, B., Butnaru, D., Willcox, K., and Bungartz, H. (2014). Localized discrete empirical interpolation method. *SIAM Journal of Scientific Computing*, 36(1). doi:10.1137/130924408.

Peherstorfer, B. and Willcox, K. (2015). Online adaptive model reduction for nonlinear systems via low-rank updates. *SIAM Journal of Scientific Computing*, 37(4). doi:10.1137/140989169.

Shin, D., Yang, D., and Choi, J. (2009). On the use of pseudo-spectral method in model reduction and simulation of active dendrites. *Computers in Biology and Medicine*, 39(4), 340–345.

Sirovich, L. (1987). Turbulence and the dynamics of coherent structures. I-III. *Quarterly of Applied Mathematics*, 45(3), 561–590.

Sorensen, M. and DeWeerth, S. (2006). An algorithmic method for reducing conductance-based neuron models. *Biological Cybernetics*, 95(2), 185–192.

Wade, J.J., McDaid, L.J., Harkin, J., Crunelli, V., and Kelso, J.A.S. (2011). Bidirectional coupling between astrocytes and neurons mediates learning and dynamic coordination in the brain: A multiple modeling approach. *PLOS ONE*, 6(12), 1–24. doi:10.1371/journal.pone.0029445.

Woo, B., Shin, D., Yang, D., and Choi, J. (2005). Reduced model and simulation of neuron with passive dendritic cable: an eigenfunction expansion approach. *Journal of Computational Neuroscience*, 19(3), 379–397.